

Figura 4.22. Valorador automático CRISON Compact Titrator Versión D.

Por otro lado, diferentes autores recomiendan el uso de técnicas complementarias a la valoración química de Boehm ya que establecen la dificultad de usarla cuando la granulometría de la muestras es muy pequeña y proponen el uso complementario de diferentes técnicas. Por ejemplo, XPS daría un valor aproximado de la composición química de las capas más superficiales del material. Otra técnica adicional sería la espectroscopía IR aunque solo puede ser aplicada a carbones altamente oxidados, es decir, de gran funcionalidad dado que las bandas de absorción no serían de suficiente intensidad.



Figura 4.23. Equipo para análisis de TPD Termo Finnigan modelo TPDR 1100 (izquierda) conectado a un analizador de masas Pfeiffer Vacuum Omnistar modelo GSD 301 O (derecha).

Aunque de todas las técnicas propuestas, Figueiredo^[96, 97] recomienda el uso de métodos de temperatura programada con la que los grupos oxigenados que se encuentran en la superficie se descomponen al calentar en forma de CO y CO₂. Así que se puede relacionar los picos obtenidos por TPD con los grupos superficiales específicos, si bien éstos pueden verse afectados por la textura del material, la velocidad de calentamiento establecida en el experimento y la geometría del sistema experimental utilizado, mediante un TPD conectado en serie con un analizador de masas (ver *Figura 4.23*).

4.3.4. Análisis de adsorción

A la hora de comprobar el comportamiento de los CA preparados, las pruebas realizadas se han basado en la adsorción de contaminantes en efluentes líquidos.

4.3.4.1. Adsorción de azul de metileno

Fundamentos

El método de adsorción de azul de metileno se basa en la isoterma de adsorción de un solo punto para azul de metileno en un medio de ácido acético diluido^[98]. El resultado se expresa en gramos de azul de metileno adsorbidos por 100 gramos de carbón.

El azul de metileno es el compuesto de mayor uso en la evaluación del poder decolorante del carbón activado y su adsorción es indicia de la presencia de macro y mesoporos debido al gran tamaño de esta molécula, la cual es aproximadamente 1.5 nm.

Equipamiento

El equipo utilizado para el análisis de muestras por colorimetría es un espectrofotómetro UV-VIS 8500 de Dinko Instruments que dispone de una lámpara de tungsteno que se utiliza para el análisis de muestras a una longitud de onda de 664.8 nm (ver *Figura 4.24*).

El análisis se ha realizado introduciendo 33.7 mg de CA en base seca con una precisión de 0.1 mg en un bote de plástico con tapa roscada de 50 ml. Posteriormente se ha añadido 50 ml de solución de azul de metileno 3.2 mM, se tapa el bote y se deja agitando la suspensión durante al menos 24 horas. Pasado este tiempo, se filtra la mezcla por gravedad con un papel de poro

medio en un vaso de precipitado limpio y seco, descartando los primeros 5 ml, y del filtrado posterior obtenido, se realizan las diluciones necesarias para que la concentración esté en el rango de medida del aparato utilizado.

La medida de la concentración de orgánico se realiza mediante el espectrofotómetro de la figura anterior, donde también se miden los blancos y los patrones. La cantidad adsorbida se calcula por diferencia entre el valor inicial y el final.

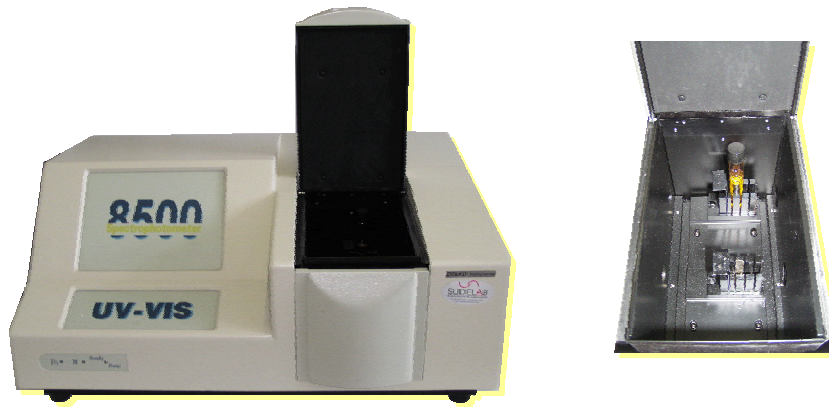


Figura 4.24. Espectrofotómetro Dinko Instruments UV-VIS 8500 y detalle de su interior.

4.3.4.2. Adsorción de yodina

Fundamentos

El número de yodo $\left(\frac{X}{M}\right)$ es un indicador relativo de la porosidad en el carbón activo aunque no da necesariamente una medida de la habilidad del carbón para absorber otras especies, como en el caso de la adsorción de azul de metileno. La adsorción de yodo se realiza con el propósito de establecer la capacidad de los carbones activados preparados por activación química, de adsorber moléculas no polares de diámetro pequeño. El número de yodo se puede utilizar como una aproximación del área superficial, en especial con el volumen de microporos^[99], para algunos tipos de carbones activados aunque su relación no puede generalizarse. Ésta varía con el cambio de materia prima del CA, las condiciones de trabajo y la distribución de volumen de poro.

Éste método se basa en la obtención de una isoterma de adsorción de tres puntos^[100, 101] que se obtiene a partir de la utilización de una solución de yodo

de concentración conocida que se pone en contacto con tres cantidades de CA bajo condiciones de trabajo específicas. Esta suspensión se filtra y se mide la concentración de yodina en la solución restante mediante espectrofotometría.

Equipamiento

El equipo utilizado para el análisis de muestras por colorimetría es un espectrofotómetro UV-VIS 8500 de Dinko Instruments (ver *Figura 4.24*) que dispone de una lámpara de tungsteno que se utiliza para el análisis de muestras a una longitud de onda de 458.4 nm.

El análisis se ha realizado pesando diferentes cantidades de CA (por ejemplo, 0.1, 0.2, 0.3, 0.4 y 0.5 g) en base seca con una precisión de 0.1 mg en un erlenmeyer de cristal limpio y seco. Posteriormente se ha añadido 50 ml de solución de yodina 0.1 N (0.05 M), se tapa el erlenmeyer con parafilm y se deja agitando la suspensión durante al menos 24 horas a oscuras. Pasado este tiempo, se filtra la mezcla por gravedad con un papel de poro medio en un vaso de precipitado limpio y seco y del filtrado obtenido, se realizan las diluciones necesarias para que la concentración esté en el rango de medida del aparato utilizado.

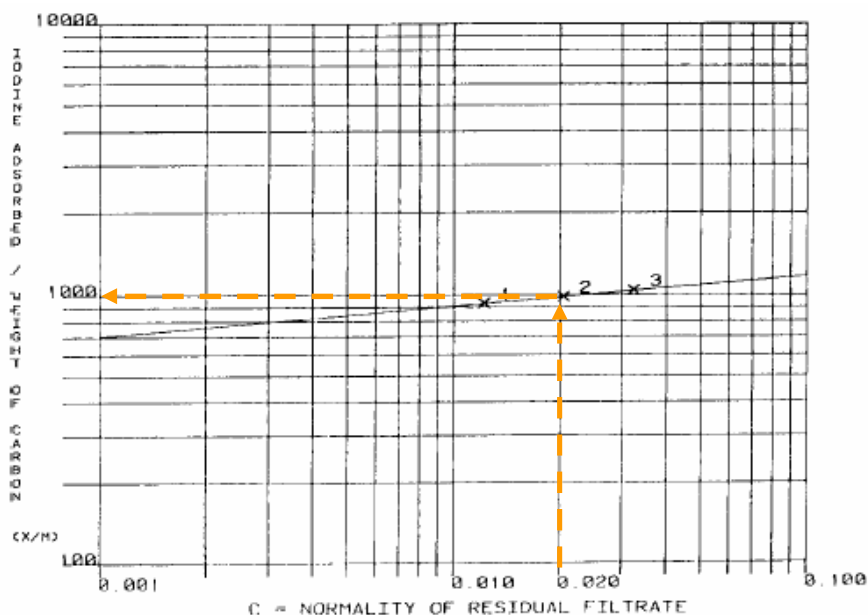


Figura 4.25. Ejemplo de isoterma de adsorción de yodo en CA^[102].

La medida de la cantidad de orgánico por gramo de CA se realiza mediante el espectrofotómetro de la *Figura 4.24*, utilizando como blanco agua MilliQ y donde también se miden los patrones de diferentes concentraciones dentro del rango de linealidad. De las muestras preparadas no solo se mide el número de yodo, sino también un parámetro llamado normalidad del filtrado residual (C). A partir de los datos de X/M y C se realiza una regresión lineal y el valor final para el número de yodo se obtiene cuando C es de $0.02N^{[102]}$, tal y como se muestra en la *Figura 4.25*.

4.3.4.3. Determinación de metales

Fundamentos

En el caso de la adsorción de metales, la técnica utilizada ha sido la absorción atómica ya que permite la determinación cuantitativa de la mayoría de los elementos de la tabla periódica en una gran variedad de muestras. La cuantificación se basa en la absorción de la luz por los átomos del metal en estado fundamental. Esta técnica está especialmente indicada para determinar elementos alcalinos, alcalinotérreos y metales pesados presentes en cualquier tipo de muestra previamente disuelta. El rango de análisis está entre tantos por cientos y partes por billón (1 mg/tonelada).

Equipamiento

El equipo utilizado para determinar la cantidad adsorbida de cobre es un sistema de Absorción Atómica Perkin Elmer 3110 (ver *Figura 4.25*) a una longitud de onda de 216.5nm.

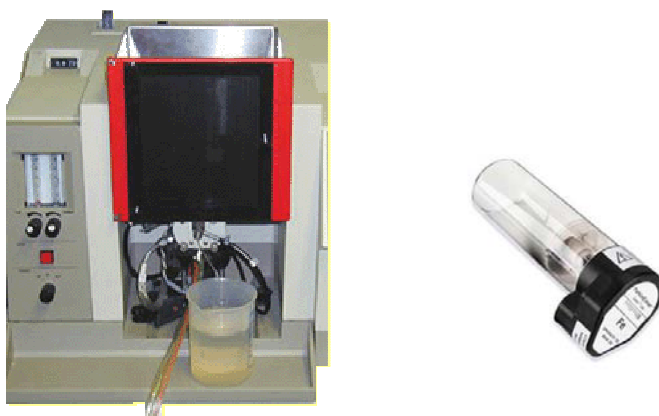


Figura 4.26. Equipo de Absorción Atómica para la determinación de cobre (II) y lámpara específica.

Los experimentos se han realizado en sistemas batch mediante la utilización de 18 erlenmeyers. Cada uno de ellos contiene 150 mg de CA en suspensión con 150 ml de agua desionizada y diferentes cantidades de cloruro de cobre (II), suministrado por Aldrich, se añaden a cada frasco. El pH inicial de cada frasco se ajusta a 5 mediante la adición de NaOH 0.1N y se deja en agitación durante 24 horas a 25°C, tal y como se muestra en la figura siguiente.



Figura 4.27. Sistema de análisis empleado para la adsorción de metales.

La concentración final de cobre se analiza mediante el equipo mencionado y la cantidad adsorbida se calcula por diferencia entre el valor inicial y el final.

4.3.4.4. Determinación de componentes orgánicos

Fundamentos

Por otro lado, también se ha analizado la adsorción^[103] de componentes orgánicos como el fenol^[4, 22, 104-162] y el benceno^[139, 162-164] mediante cromatografía de líquidos. Estos compuestos se han escogido como representantes de los contaminantes orgánicos más comunes en los efluentes industriales. En la actualidad, esta técnica de separación es la más extendida utilizada debido a su versatilidad y amplio campo de aplicación. Los componentes de la muestra, previamente disueltos en un disolvente adecuado (fase móvil), son forzados a atravesar la columna cromatográfica gracias a la aplicación de altas presiones. El material interno de la columna, fase estacionaria, está constituido por un relleno capaz de retener de forma selectiva los componentes de la mezcla. La resolución de esta separación depende de la interacción entre la fase estacionaria y la fase móvil, pudiendo

ser manipulada a través de la elección de diferentes mezclas disolventes y distintos tipo de relleno. Como resultado final los componentes de la mezcla salen de la columna separados en función de sus tiempos de retención en lo que constituye el cromatograma. A través del cromatograma se puede realizar la identificación cualitativa y cuantitativa de las especies separadas.

El campo de aplicación de esta técnica es muy extenso, pudiendo tratar productos farmacéuticos (antibióticos, sedantes, esteroides, analgésicos), bioquímicos (aminoácidos, proteínas, carbohidratos, lípidos), alimentarios (edulcorantes artificiales, antioxidantes, aditivos), contaminantes (plaguicidas, herbicidas, fenoles, PCBs), en química forense (drogas, venenos, alcohol en sangre, narcóticos) y en medicina clínica (ácidos biliares, metabolitos de drogas, extractos de orina, estrógenos).

Equipamiento

En este caso, el análisis se ha llevado a cabo en un cromatógrafo de líquidos de alta precisión Agilent 1100 Series dotado de una columna Hypersil ODS 250 mm y utilizando como fase móvil acetonitrilo/agua en una proporción 65/35. A estas condiciones, los tiempos de residencia de los compuestos orgánicos estudiados son 1.5 minutos para el fenol y 2.5 minutos para el benceno.



Figura 4.28. HPLC: Cromatógrafo de líquidos Agilent 1100 Series.

Adsorción de componentes orgánicos

Para realizar este análisis se ha añadido 10 mg de CA a un bote de cristal con tapón roscado que contenía 10 ml de una disolución de 100 ppm de benceno o fenol preparada con agua ultrapura procedente de un equipo de Milli-Q Millipore alimentado con agua destilada. Cada muestra se preparará por triplicado así como también se preparará por triplicado un blanco sin CA.

Cada frasco se tapa bien y se deja agitando durante 48 horas, tiempo suficiente para alcanzar el equilibrio, a una temperatura constante de 25°C en un baño térmico. Las muestras se colocan perpendicularmente sobre un eje de rotor que gira a una velocidad de 2 rpm. La temperatura se controla mediante un regulador electrónico digital de temperatura P>Selecta modelo Digiterm 100.

Posteriormente, se coge muestra suficiente con ayuda de una jeringuilla y una aguja y se pasa a través de un filtro de celulosa regenerada a un vial de 0.45 μm de tamaño de poro, el cual se tapa y se etiqueta. La medida de la concentración de orgánico se realiza mediante HPLC, donde también se miden los blancos y los patrones. La cantidad adsorbida se calcula por diferencia entre el valor inicial y el final.

Cinéticas de adsorción

Previamente al análisis de adsorción de fenol y benceno, se han realizado estudios cinéticos para determinar el tiempo de adsorción mínimo necesario para alcanzar el equilibrio. La preparación de las muestras se ha llevado a cabo de manera similar a los análisis de adsorción. En este caso, se preparan diferentes botes de cristal que contienen 10 mg de CA y 10 ml de la solución de orgánico recién preparada, tal y como se ha descrito anteriormente.

Todas las muestras se dejan en agitación durante un tiempo determinado hasta un máximo de 7 días y posteriormente la muestra se trata para el análisis, tal y como se ha descrito anteriormente. El equilibrio para el fenol se alcanza en 8 horas mientras que para el benceno, el equilibrio se alcanza a las 2 horas.

Isotermas de adsorción

De igual manera a los análisis de cinética de adsorción, se realizan las isotermas de los dos compuestos orgánicos estudiados. Para ello, diferentes cantidades de adsorbato (1-20 mg) se mezclan con 10 ml de solución contaminante recién preparada de fenol o benceno, a una concentración 100 ppm. Los tubos se tapan y se ponen en agitación durante 8 horas, asegurando así alcanzar el equilibrio establecido mediante los análisis cinéticos, a una velocidad rotatoria de 2 rpm. Una vez transcurrido el tiempo establecido, se toma muestra de cada uno de los botes de cristal y se analiza tal y como se ha realizado anteriormente, en los análisis de adsorción de componentes orgánicos, mediante HPLC.

4.4. Aplicaciones de los carbones activados

Una vez caracterizados, se pueden emplear en el campo de aplicación más adecuado. En este caso, ya que los CA obtenidos son microporosos, se usarán con el objetivo de adsorber metales pesados como el cobre y NOC de efluentes líquidos. Los NOC escogidos han sido fenol y benceno ya que en las últimas décadas la calidad de muchas aguas se ha visto afectadas por la creciente producción de productos químicos tales como pinturas, adhesivos, plásticos, etc. de los que se generan residuos que contaminan, no solo las aguas superficiales, sino también las subterráneas y estos dos componentes son representativos de esta familia de contaminantes.

Por otro lado, el CA también se ha utilizado para obtener membranas poliméricas compuestas, etapa previa a la obtención de reactores de membranas enzimáticos, utilizando el carbón inmovilizado en la matriz polimérica para adsorber enzimas directamente, o a través de un metal (cobre en este caso), considerando como base la técnica de cromatografía de afinidad con ión metálico inmovilizado (IMAC)^[165]. A pesar que existen muchos ámbitos de aplicación para este tipo de membranas, en este trabajo se han utilizado para obtener y separar azúcares de muy bajo peso molecular (cerca al del monómero) a partir de azúcares de tamaño superior.

5. DISCUSIÓN DE RESULTADOS

Una vez preparados y caracterizado los CA (Etapa 1 y 2) se han preparado una serie de artículos que han sido enviados a diferentes publicaciones. Posteriormente, y a partir de la caracterización realizada, los CA preparados en estas dos etapas se emplean en campos determinados, como la adsorción de componentes orgánicos en sistemas líquidos, y en casos más específicos, como por ejemplo, para la obtención de membranas poliméricas donde se retiene un enzima específica.

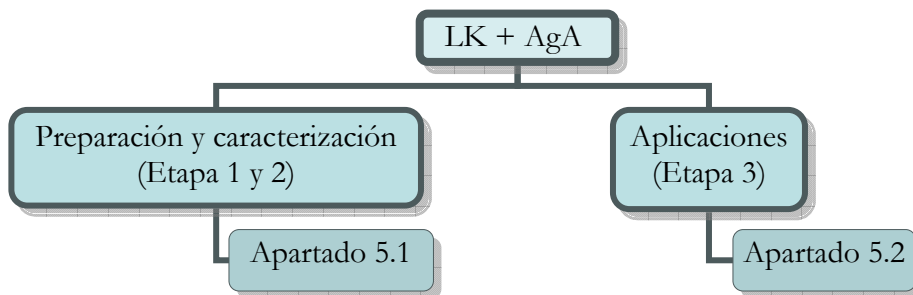


Figura 5.1. Resumen de los reports realizados a partir de la obtención de datos en las etapas 1, 2 y 3.

La lignina Kraft es un material poco utilizado en la preparación de CA, ya que normalmente se utilizan materiales que contienen este polímero pero no por separado. Por esta razón, el estudio de la activación química de la lignina es novedoso y se hace necesario el conocimiento, no tan sólo las características del producto obtenido, sino también por qué tienen lugar y de esta manera prever las características finales del producto con las condiciones de operación necesarias para obtenerlo.

En el caso de la activación química de la lignina Kraft con ácido fosfórico, en primer lugar es necesario conocer los fenómenos que tienen lugar durante la pirólisis y saber qué tipo de porosidad se desarrolla en la obtención de AC-P. En este caso, los estudios en termobalanza son muy útiles y gracias a los datos experimentales obtenidos se ha podido proponer un modelo cinético²⁶ que se ajusta a los escasos datos que se encuentran en la literatura.

Paralelamente al estudio cinético, es necesario conocer como afectan las condiciones de preparación de los AC-P en sus propiedades físico-químicas finales^{27,28}. Este punto es básico para el desarrollo de los objetivos que presenta esta memoria ya que poder prever las condiciones de operación en

²⁶ Montané, D.; Torné-Fernández, V.; Fierro, V.; Activated carbons from lignin: kinetic modelling of the pyrolysis of Kraft lignin activated with phosphoric acid. Chemical Engineering Journal, 2005. 106:p.1-12. (Ver *Apartado 5.1.1*).

²⁷ Fierro, V.; Torné-Fernández, V.; Montané, D.; Celzard, A.; Study of the decomposition of Kraft lignin impregnated with orthophosphoric acid. Thermochimica acta, 2005. 433:p.142-148. (Consultar *Apartado 5.1.2*).

²⁸ Fierro, V.; Torné, V.; Montané, D.; Salvadó, J.; Activated carbons prepared from Kraft lignin by phosphoric acid impregnation. Póster. Carbon. Oviedo (España). 2003. (Ver *Anexo B*).

el proceso de descomposición térmica de la lignina Kraft activada con ácido fosfórico a partir de las propiedades finales deseadas, conlleva un ahorro de tiempo y recursos muy importante. En concreto, parámetros tan importantes como el rendimiento a carbón, el área superficial y la distribución de tamaño de poros²⁹ son aspectos determinantes a la hora de escoger un sólido poroso para una aplicación determinada.

Por otro lado, las características de la materia prima que se utilizan también pueden afectar a las propiedades finales del AC-P³⁰. En concreto, el efecto de las cenizas³¹ que contiene la lignina Kraft, tal y como se suministra, en comparación con el uso de lignina Kraft desmineralizada, es decir, después de proceder a un pretratamiento ácido con el fin de disminuir el contenido en cenizas formadas por sales, afecta a su polimerización y puede reducir la interacción con el agente activante.

En el desarrollo de carbones activados con hidróxido de potasio^{32,33} y sodio³⁴ se ha desarrollado un incremento de interés, por esta razón estudiar la posibilidad de preparar CA microporosos a partir de lignina Kraft desmineralizada e hidróxidos estudiando, como en el caso anterior, el efecto de las condiciones de operación, es importante desde el punto de vista de desarrollar otra vía de producción de CA sin utilizar ácidos.

²⁹ Fierro, V.; Torné-Fernández, V.; Celzard, A.; Kraft lignin as a precursor for microporous activated carbons prepared by impregnation with ortho-phosphoric acid: synthesis and textural characterisation. *Microporous and mesoporous materials*, 2006. 92(1-3):p.243-250. (Consultar *Apartado 5.1.3*).

³⁰ Fierro, V.; Torné-Fernández, V.; Celzard, A.; Montané, D.; Influence of the demineralisation on the chemical activation of Kraft lignin with orthophosphoric acid. Enviado a *Journal of Hazardous Materials* (Mayo 2006). (Consultar *Apartado 5.1.4*).

³¹ Fierro, V.; Torné, V.; Celzard, A.; Influence of the ash content on the microporosity of activated carbons derived from Kraft lignin. Póster. *Carbon*. Corea. 2005. (Ver *Anexo G*).

³² Fierro, V.; Torné-Fernández, V.; Celzard, A.; Highly microporous carbons prepared by activation of Kraft lignin with KOH. *Studies in Surface Science and Catalysis*, 2005. 607-614. (Consultar *Apartado 5.1.5*).

³³ Fierro, V.; Torné-Fernández, V.; Celzard, A.; Highly microporous carbons prepared by activation of Kraft lignin with KOH. Póster. *7th International Symposium on the characterization of porous solids*. Aix-en-Provence (Francia). 2005. (Ver *Anexo E*).

³⁴ Fierro, V.; Torné-Fernández, V.; Celzard, A.; Methodical study of the chemical activation of Kraft lignin with KOH and NaOH. Enviado a *Microporous and Mesoporous Materials*, 2006. (Consultar *Apartado 5.1.6*).

Finalmente, una vez se tienen caracterizados los CA preparados por diferentes métodos, estos se pueden aplicar en el campo más adecuado. La principal aplicación de estos carbones está en la adsorción de diferentes tipos de compuestos contaminantes (componentes metálicos^{35,36,37}, componentes orgánicos de diferente polaridad^{38,39}, etc.) en sistemas líquidos ya que los carbones preparados son básicamente microporosos de áreas superficiales altas.

Sin embargo, estos carbones pueden tener otro campo de aplicación como es el de aditivo en membranas⁴⁰ para la obtención de reactores enzimáticos de membrana (EMR), a partir de una matriz polimérica (polisulfona) y la incorporación de carbón activado, el cual se usa para adsorber la enzima directamente o a partir de un metal, considerando las bases de la técnica IMAC^[165].

Por último, la experiencia ganada en el desarrollo de esta tesis ha permitido trabajar en otros trabajos que han consistido en la caracterización de carbones para la purificación de xilo-oligosacáridos⁴¹. Éste producto tiene

³⁵ Fierro, V.; Torné, V.; Montané, D.; García-Valls, R.; Removal of Cu (II) from aqueous solutions by adsorption on activated carbons prepared from Kraft lignin. Póster. Carbon 2003. 6-10 Julio, Oviedo (España). (Consultar *Apartado 5.2.1*, ver *Anexo C*).

³⁶ Novellon, E.; Fierro, V.; Torné, V.; García-Valls, R.; Montané, D.; Use of Kraft lignin for Cu (II) removal in industrial water. Póster. 9th Mediterranean Congress. Barcelona (Catalunya). 2002. (Ver *Anexo A*)

³⁷ Nastrunisku, G.; Fierro, V.; Torné, V.; García-Valls, R.; Montané, D.; Uptake of Cu (II) and Zn from aqueous solutions by Kraft lignin. Póster. 4th European Congress in Chemical Engineering. Granada (España). 2003. (Ver *Anexo D*).

³⁸ Torné-Fernández, V., Mateo, J. M., Montané, D., Fierro, V.; Optimization of the synthesis of highly microporous carbons by chemical activation of Kraft lignin with NaOH. Enviado a Chemical Engineering Journal, 2006. (Consultar *Apartado 5.2.2*).

³⁹ Torné-Fernández, V., Fierro, V.; Sorption study of organic compounds on highly microporous carbons prepared from Kraft lignin. Enviado al journal Adsorption Science and Technology, 2006. (Consultar *Apartado 5.2.3*).

⁴⁰ Torras, C.; Torné, V.; Fierro, V.; Montané, D.; Garcia-Valls, R. ; Polymeric composite membranes based on carbon/PSf. Journal of membrane science, 2006. 273:p. 38-46. (Consultar *Apartado 5.2.4*, ver *Anexo F*).

⁴¹ Montané, D.; Nabarlantz, D.; Martorell, A.; Torné-Fernández, V.; Fierro, V.; Removal of lignin and associated impurities from xylo-oligosaccharides by activated carbon adsorption. Industrial Engineering Chemistry Research, 2006. 45:p. 2294-2302. (Consultar *Apartado 5.2.5*).

gran importancia ya que deriva de hemicelulosas ricas en xilano que son carbohidratos con un alto potencial en aplicaciones en productos de alimentación y farmacéuticos. Esta metodología pretende ser aplicada en los CA preparados para esta tesis una vez se optimice, debido a la poca cantidad de CA que se obtiene en cada pirólisis.

5.1. Preparación y caracterización de carbones activados

A continuación se presentan seis artículos publicados y enviados a diferentes revistas que tratan de la preparación y caracterización de carbones procedentes de lignina Kraft y activados químicamente con ácido fosfórico, hidróxido de sodio e hidróxido de potasio a diferentes condiciones de operación.

5.1.1. Activated carbons from lignin: kinetic modeling of the pyrolysis of Kraft lignin activated with phosphoric acid

Este artículo se ha publicado en el Chemical Engineering Journal en 2005 en el volumen 106, páginas 1 a 12.



Activated carbons from lignin: kinetic modeling of the pyrolysis of Kraft lignin activated with phosphoric acid

Daniel Montané*, Vanessa Torné-Fernández, Vanessa Fierro

Department of Chemical Engineering-ETSEQ, Rovira i Virgili University, Av. Països Catalans 26, E-43007 Tarragona, Catalunya, Spain

Received 26 April 2004; received in revised form 19 October 2004; accepted 4 November 2004

Abstract

A phenomenological kinetic model has been developed for the pyrolysis at low heating rates of lignin activated with phosphoric acid. The model is based on thermogravimetry (TG) and differential thermogravimetry (DTG) data from pyrolysis experiments and assumes that lignin carbonization proceeds through a set of pseudo-first-order reactions. These reactions are a simplified description of the multiple reactions involved in the process. TG experiments were performed in nitrogen atmosphere for lignin (L) impregnated with 85% phosphoric acid (PA) at mass ratios (PA:L) from 1.0:1.0 to 1.75:1.0, a typical heating rate of 10 °C/min and a maximum carbonization temperature of 650 °C, including isothermal stages at 150 and 300 °C in the temperature programs for some of the experiments. Analysis of the TG and DTG curves led to a kinetic model that includes an initial reaction step between lignin and phosphoric acid, water formation from the dehydration of the excess of phosphoric acid to P₂O₅, pyrolysis of lignin to carbon and volatiles, evaporation of water and P₂O₅ and finally, partial volatilization of the carbon to light gases. Activation energies and the other parameters of the model were adjusted from experimental data. Activation energies were 26.0 kJ/mol for water desorption, 72.0 kJ/mol for the dehydration of phosphoric acid to phosphoric pentoxide, 95.0 kJ/mol for the volatilization of P₂O₅, 47.7 kJ/mol for the carbonization of the activated lignin and 106.3 kJ/mol for the pyrolytic release of light gases from activated carbon. The model provides a good representation of the thermograms regardless of the phosphoric acid to lignin ratio and the temperature profile along the reaction.

© 2004 Elsevier B.V. All rights reserved.

Keywords: Lignin; Activated carbon; Phosphoric acid; Pyrolysis; Kinetics; Thermogravimetric analysis

1. Introduction

Activated carbons are adsorbents that are used industrially in multiple processes for product separation and purification, and for the treatment of liquid and gaseous effluents. Their versatility allows a wide range of uses if their pore size distribution and surface properties are properly tailored, and new applications are being developed in areas such as pollution prevention, supported catalysts and the storage of gaseous fuels such as natural gas and hydrogen. Activated carbons are produced from a wide variety of carbonaceous materials, including wood and agriculture by-products [1], but the expanding market for activated carbons has prompted inter-

est in finding complementary sources of carbonaceous precursors for their manufacture. Using carbonaceous residues and by-products from existing industrial processes as feedstock for producing activated carbons is an attractive strategy that may help reduce costs through process integration. Among several possibilities, lignin, produced as a residual material in the manufacture of cellulose pulps, offers strong potential because it is available in high amounts at low cost. Lignin is the most abundant natural polymer after cellulose. Typically, it represents around 20–30% of the mass of dry wood and is nowadays produced in huge amounts as a by-product in the production of high-quality cellulose pulps, mainly in the Kraft pulping process. In this process, lignin is used as fuel to provide steam for the plant, which also allows the recovery of the pulping chemicals (NaOH and Na₂S). The trend towards larger plant capacities and the op-

* Corresponding author. Tel.: +34 977 559 652; fax: +34 977 558 544.
E-mail address: dmontane@etseq.urv.es (D. Montané).

Table 1
 Lignin analysis (wt. %)

Proximate analysis (wt. %, wet basis)		Ultimate analysis (wt. %, ash and moisture free)	
Moisture	14.45	Carbon	59.46
Ash	9.50	Hydrogen	5.07
Volatile matter	44.93	Nitrogen	0.05
Fixed carbon ^a	31.12	Sulfur	2.15
		Oxygen ^a	33.27

^a Estimated by difference.

timization of the pulping process to improve cost effectiveness have led to the plants producing more by-product lignin than the amount that is needed to cover their energy consumption. Using Kraft lignin as raw material for chemicals has therefore attracted considerable attention. Several applications for the lignin obtained from pulping processes have been considered. One of its main uses so far has been as a phenol substitute in the formulation of phenol–formaldehyde resins and adhesives, but one of the main areas for possible applications for by-product lignin is in the preparation of activated carbons. The physical activation with CO₂ of pyrolyzed lignins [2,3], as well as chemical activation of lignin with ZnCl₂ [4], have been studied, but the use of ZnCl₂ is declining due to its environmental impact [5], and phosphoric acid is the preferred activating agent. However, the activation of lignin with phosphoric acid has not been widely investigated, though maximum surface areas of above 1300 m²/g have been reported [6]. We recently studied the characteristics of the carbons obtained from Kraft lignin activated with phosphoric acid at several process conditions and showed that carbons with high surface areas and good properties can be obtained [7]. In this paper, we study the rates of carbonization of Kraft lignin activated with phosphoric acid in a thermobalance and propose and test a phenomenological kinetic model with the experimental data.

Table 2
 Experimental conditions used for the TGA experiments

Run ID	H ₃ PO ₄ (85%) to lignin mass ratio	Initial temperature (°C)	Heating rate (°C/min)	First stage		Second stage		Third stage	
				T (°C)	Time (min)	T (°C)	Time (min)	T (°C)	Time (min)
Exp #10/3	1.4	25	10	650	120	–	–	–	–
Exp #10/4	1.4	25	10	650	120	–	–	–	–
Exp #10/5	1.4	25	10	650	120	–	–	–	–
Exp #2	1.4	25	10	150	15	650	0	–	–
Exp #3	1.4	25	10	150	30	650	30	–	–
Exp #5	1.4	25	10	150	60	650	120	–	–
Exp #13	1.4	25	10	150	60	650	120	–	–
Exp #18	1.4	25	10	300	60	650	120	–	–
Exp #20	1.4	25	10	150	60	300	60	650	120
Exp #21	1.4	25	10	300	60	500	60	750	60
Exp #24	1.4	150	150	650	120	–	–	–	–
Exp #10 (L/P 1:1.0)	1.0	25	10	650	30	–	–	–	–
Exp #14 (L/P 1:1.4)	1.4	25	10	600	120	–	–	–	–
Exp #18 (L/P 1:1.75)	1.75	25	10	650	120	–	–	–	–

2. Experimental

A sample of Kraft lignin was obtained from Lignotech Ibérica S.A. (Spain) and used to prepare activated carbons as received (see Table 1 for composition). Elemental analysis was performed in a EA1108 Carlo Erba analyzer and the proximate analysis was developed according to ISO standards for moisture (100 °C in air), volatile matter (900 °C in nitrogen atmosphere) and ash (incineration at 815 °C in air).

Phosphoric acid (85% solution, Panreac, Spain) was used as activating agent. Lignin and phosphoric acid were mixed at the desired ratio and the mixture was left for 1 h to allow a complete impregnation of the lignin [8]. A small sample (around 30–50 mg) of the mixture was then transferred to the thermobalance (Perkin-Elmer TGA-7), where pyrolysis was carried out in nitrogen at a constant flow rate of 50 mL/s. Table 2 lists all the other specific conditions for the experiments, which were performed randomly except for a first series, which was performed to establish the reproducibility of the TG results.

3. Results and discussion

Our first set of experiments tested the reproducibility of our experimental procedure. Fig. 1 shows the thermograms (*f* versus *t*) and the differential thermograms (*df/dt* versus *t*) for replicated experiments on the carbonization of a sample of lignin impregnated with a phosphoric acid to lignin mass ratio (PA/L) of 1.4, a heating rate of 10°/min and a final temperature of 650 °C for 120 min (experiments #10/3, #10/4 and #10/5 in Table 2). Since our experiments included isothermal periods, either at the end of the heating ramp or intercalated in it, we preferred time instead of temperature as the independent variable for our calculations. The average value for the final mass fraction was 0.384 ± 0.014 (95% probability level), which shows the good reproducibility of the ex-

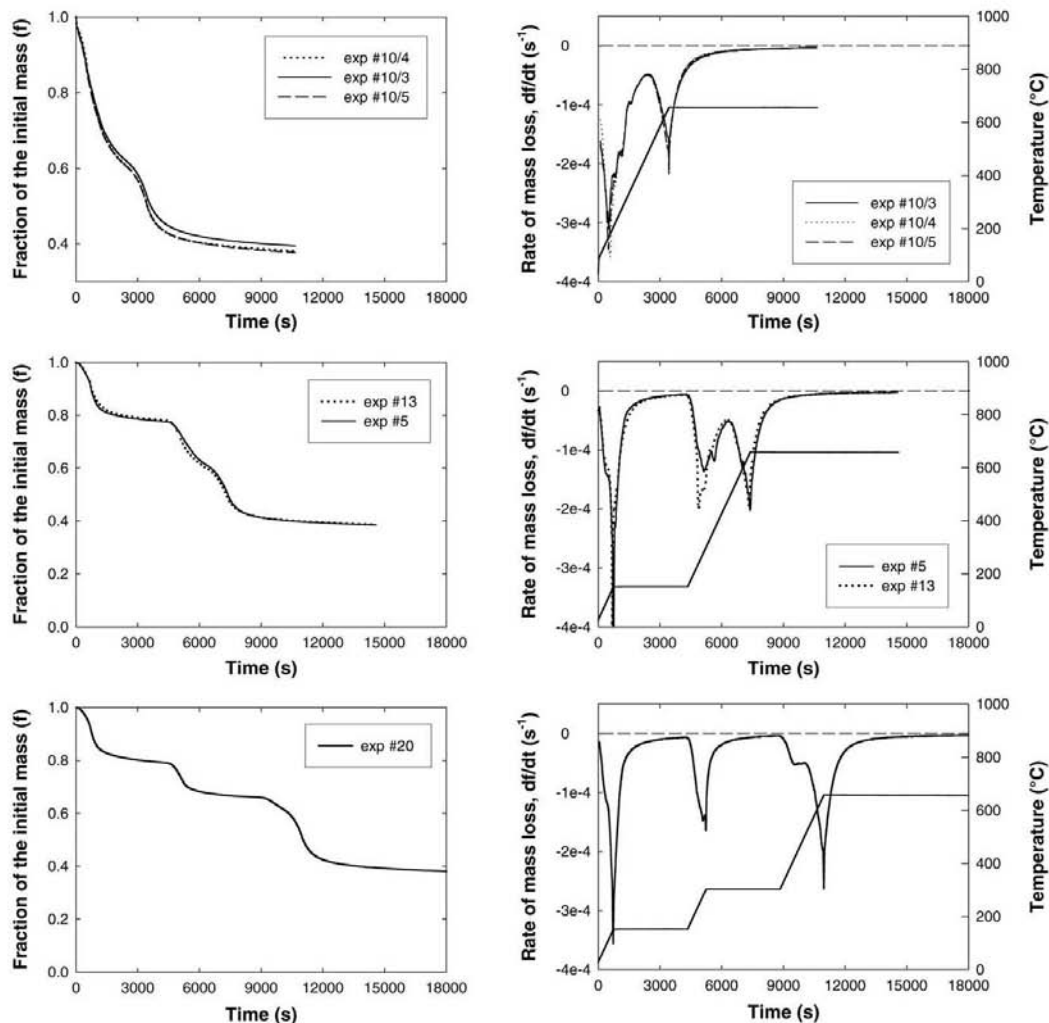


Fig. 1. Effect of the addition of intermediate isothermal stages on the final solid yield and the TG and DTG curves for experiments #5, #10/4 and #20 (experimental conditions listed in Table 2).

periments. The differential thermograms also show excellent agreement among the three experiments throughout the reaction time, since the values of the maximum rates of mass loss and the time at which they are observed are almost identical for the three runs. The differential thermogram shows two peaks for the rate of mass loss. The first starts at low temperature, reaches the maximum rate at around 175–180 °C and extends to 450 °C. The second peak starts at around 500 °C and reaches the maximum rate of mass loss when the isothermal segment at 650 °C starts.

Yoon et al. [9] reported an increase in carbon yield when the sample was maintained at constant temperature for a cer-

tain time once the volatilization of the sample had started. Other studies, however, reported that the carbon yield did not change when intermediate isothermal periods were included during the pyrolysis of viscose rayon cloth [10] and apple pulp [11]. We performed experiments #5 and #13, under the same conditions as #10/3, #10/4 and #10/5 but with an isothermal segment at 150 °C for 60 min. Again, reproducibility was excellent for the TG and DTG curves (Fig. 1). The mass fraction remaining at the end of the experiments was 0.386 ± 0.002 , which is equivalent to that of the experiments without intermediate isothermal period. We may therefore conclude that including isothermal periods does not signif-

icantly changes the final yield of solid. However, including intermediate isothermal stages proved valuable because it revealed that the peaks of the rate of mass loss in the DTG were the result of the superposition of several reactions. For example, if we compare the DTG plots for experiments #10/4 and #5 we can see that the broad peak observed during the heating period in experiment #10/4 splits into two different peaks when an intermediate isothermal period at 150 °C is added. The new peak shows the maximum rate of mass loss at 350–400 °C, but it appears also to be the result of the superposition of two reactions. This is confirmed by experiment #20, which adds two isothermal periods — one at 150 °C for 60 min and another at 300 °C for 60 min — and shows the existence of four maximums in the rate of mass loss along the thermogram. This experiment also had a yield of residual solid of 0.381, which confirmed that including intermediate isothermal stages has no significant effect on the final mass fraction if the same final temperature of carbonization is achieved.

4. Modeling of lignin pyrolysis

Several models are available in the bibliography for the kinetics of the thermal decomposition of biomass and its fractions. The most usual approach starts with the assumption that the components of biomass (cellulose, hemicellulose and lignin) react simultaneously and independently of the others through a set of parallel reactions [12–15]. When applied to lignin activated with phosphoric acid, the model is reduced to two parallel and independent reaction processes: the volatilization of the water present in the sample and the carbonization of the phosphoric acid-activated lignin (PL) into activated carbon and volatiles. Water comes from the phosphoric acid solution and the moisture of lignin. This system is described mathematically by Eqs. (1)–(5), where m_{0LP} and m_{0W} are the initial masses of PL mixture and water, m_{LP} and m_W the actual masses of PL and water at a point along the experiment, m_{∞} the residual mass of solid at the end of the thermogram, f the fraction of the initial mass remaining as solid, f_{LP} and f_W the fractions of the initial mass of phosphoric-activated lignin and water, f_{LP_0} and f_{W_0} the same at the beginning of the experiment, α_{LP} and α_W the degrees of transformation for activated lignin and water, and k_{LP} and k_W Arrhenius rate constants for the volatilization of activated lignin and water.

Water volatilization was assumed to be first-order. Some thermogravimetry studies on lignin pyrolysis propose a first-order reaction process [15–17], but most studies conclude that reaction orders are higher [13,14,18,19]. We therefore assumed that the devolatilization of activated lignin may not be first-order and included the reaction order for activated lignin (α_{LP}) as one of the parameters to be optimized from experimental data, together with the activation energies and the frequency factors. A convenient least-squares objective function to calculate the optimal values of these parameters when

using several thermograms, which may combine isothermal and non-isothermal stages, is presented in Eq. (6) for p thermograms with $n(i)$ data points each. f_{ij}^{exp} are the measured values of f , and f_{ij}^{cal} are those calculated with Eqs. (3)–(5) and numerical integration of Eqs. (1) and (2):

$$\frac{d\alpha_{LP}}{dt} = k_{LP}(1 - \alpha_{LP})^{\alpha_{LP}} \quad \text{with} \quad \alpha_{LP} = \frac{m_{0LP} - m_{LP}}{m_{0LP} - m_{\infty}} \quad (1)$$

$$\frac{d\alpha_W}{dt} = k_W(1 - \alpha_W) \quad \text{with} \quad \alpha_W = \frac{m_{0W} - m_W}{m_{0W}} \quad (2)$$

$$f_{LP} = f_{LP_0} - \alpha_{LP}(f_{LP_0} - f_{\infty}) \quad (3)$$

$$f_W = f_{W_0}(1 - \alpha_W) \quad (4)$$

$$f = f_{LP} + f_W \quad (5)$$

$$F = \sum_{i=1}^p \left(\frac{\sum_{j=1}^{n(i)} (f_{ij}^{cal} - f_{ij}^{exp})^2}{n(i)} \right) \quad (6)$$

Fig. 2 compares the thermograms and the differential thermograms recorded for experiments #10/4, #5 and #20 with those calculated with the best-fit values of the model parameters. The model describes the general trends of the thermograms qualitatively but shows large discrepancies with the experimental results, especially when two intermediate isothermal stages are included in the thermogram (experiment #20). We may therefore conclude that a better description of the interactions between lignin and phosphoric acid has to be incorporated into the model.

Analysis of the TG and DTG plots in Fig. 1 reveals some characteristic trends of the pyrolysis of lignin in the presence of phosphoric acid. Since water will evaporate at the lower temperature, the broad peak observed in the DTG between 100 and 450 °C in experiments #10/3, #4, #5 is not only caused by water evaporation but also by the decomposition of lignin and phosphoric acid. Water comes from the phosphoric acid solution, the moisture in lignin and from reactions of lignin and phosphoric acid at low temperature. In the presence of PA, lignin reacts through cleavage of the aryl-ether bonds, the formation of ketone groups, condensation and dehydration [20]. Pyrolysis of lignin in the presence of phosphoric acid shows that CO and CO₂ begin to evolve as volatile products at a temperature as low as 100 °C [21]. The inclusion of an isothermal stage at 150 °C for 60 min (experiments #5 and #20) shows that only 20% of the initial mass volatilizes at this temperature. This is attributed to the release of water and light compounds from lignin degradation by the action of phosphoric acid. When a second isothermal stage is included at 350 °C for 60 min (experiment #20), the total mass loss reaches 34%. The peak at 240–320 °C in the DTG curve for experiments #5 and #13 is attributed to the release of organic volatiles formed during the carbonization of the activated lignin. This peak is overlapped with the peak of water when no intermediate isothermal stage is used (experiments #10/3, #4, #5). When the sample is heated at 650 °C for 2 h, the final mass loss is around 62% for all experiments. The

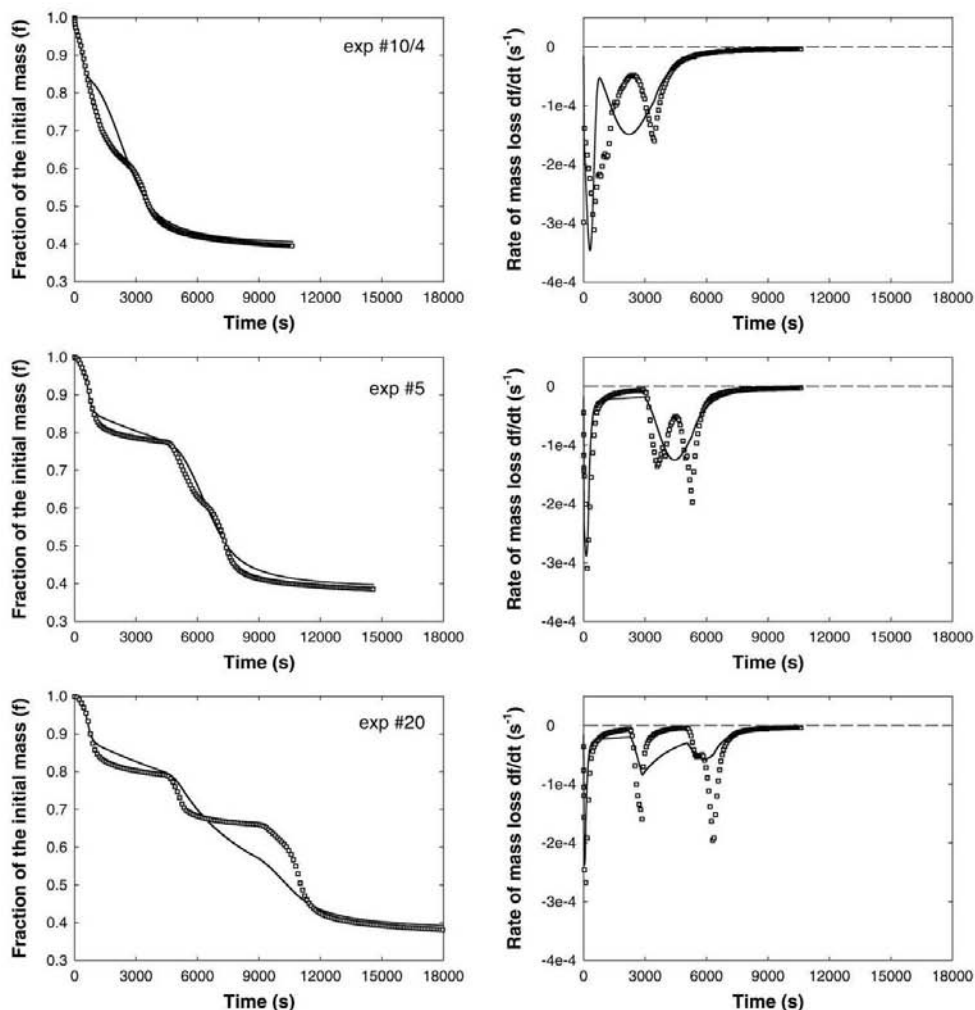


Fig. 2. Comparison between the experimental TG and DTG curves (□) and those calculated with the two parallel reactions kinetic model (–), Eqs. (1)–(5), for experiments #5, #10/4 and #20. (Experimental conditions listed in Table 2. For better visualization, only 1 data point out of 20 is plotted in the experimental TG and DTG curves.)

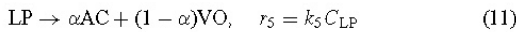
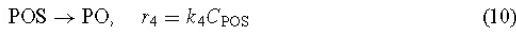
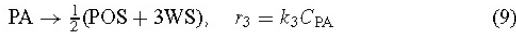
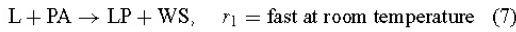
high degree of mass loss between 350 and 650 °C cannot be attributed to volatile matter from lignin alone since the rate of lignin pyrolysis reaches a maximum in the temperature interval from 300 to 370 °C [14,15]. The behavior of phosphoric acid at elevated temperature also has to be accounted for. The experiments presented in Fig. 1 were performed at a phosphoric acid-to-lignin mass ratio of 1.4:1, which exceeds the minimum ratio of 1.0:1.0 required to activate lignin completely [8]. As the temperature of the sample increases, the excess phosphoric acid is converted to pyrophosphoric acid ($H_4P_2O_7$) by condensation and dehydration. Extended heating forms polyphosphoric acid ($H_{n+2}P_nO_{3n+1}$), which

finally decomposes to form P_2O_5 , which sublimates above 300 °C and melts and vaporizes at 580–585 °C [22]. This temperature is very close to the peak observed at 650 °C in the DTG curves, which is therefore attributed to the volatilization of the P_2O_5 .

4.1. Development of a new kinetic model for the pyrolysis of lignin activated with phosphoric acid

Qualitative interpretation of the thermograms leads us to the development of a kinetic model that accounts for the observed phenomena during the pyrolysis of lignin in the pres-

ence of phosphoric acid. The process was modeled with the reaction scheme described by Eqs. (7)–(12). Eq. (7) is the formation of a complex (LP) between lignin (L) and phosphoric acid (PA) through linkage of the phosphoric group to a reactive site in lignin. Based on experimental evidence we determined that this process finishes in 1 h at room temperature [8]. Therefore, this reaction was complete before the thermal treatment was started. Eq. (8) is the drying of the sample through water (WS) evaporation. Eq. (9) accounts for the conversion of the excess phosphoric acid to P_2O_5 (POS) when water is completely removed, and Eq. (10) describes the evaporation of POS. Finally, pyrolysis of the lignin–PA complex yields activated carbon (AC) and volatiles (VO), as described by Eq. (11). The parameter α indicates the mass fraction converted to activated carbon, and $(1 - \alpha)$ indicates the mass fraction converted to volatiles during carbonization. Eq. (12) describes the partial volatilization of the activated carbon through slow pyrolysis to yield light gases (GA). All reaction rates were assumed to be first-order for each reactant.



Assuming that the reacting solid has homogeneous properties, individual mass balances are developed for each component of the solid:

$$\frac{df_{WS}}{dt} = -k_2 f_{WS} + \frac{3}{2} k_3 \frac{MW_{WS}}{MW_{PA}} f_{PA} \quad (13)$$

$$\frac{df_{PA}}{dt} = -k_3 f_{PA} \quad (14)$$

$$\frac{df_{PO}}{dt} = -k_4 f_{PO} + \frac{1}{2} k_3 \frac{MW_{PO}}{MW_{PA}} f_{PA} \quad (15)$$

$$\frac{df_{LP}}{dt} = -k_5 f_{LP} \quad (16)$$

$$\frac{df_{AC}}{dt} = \alpha k_5 f_{LP} - k_6 f_{AC} \quad (17)$$

$$\alpha' = \alpha \frac{MW_{AC}}{MW_{LP}} \quad (18)$$

where f_j denotes the mass fraction of species j referred to the initial mass of the sample (M_0), MW_j is the molar mass of species j , and the rate of decrease of the fraction of the initial mass that remains in the solid (df/dt) is obtained from Eq. (20). All the rate constants were assumed to follow the Arrhenius relationship Eq. (21).

$$f_j = \frac{M_j}{M_0} \quad (19)$$

$$\frac{df}{dt} = \frac{1}{M_0} \sum_{j=1}^5 \frac{dM_j}{dt} \quad (20)$$

$$k_i = k_{0i} \exp\left(-\frac{E_i}{RT}\right) \quad (21)$$

The initial mass-fraction composition of the sample was calculated from the amounts of phosphoric acid and lignin, the moisture content of the latter, and accounting for the water originated through reaction (1) (Eqs. (22)–(24))

$$f_{PA,0} = \frac{\left(\text{mass of anhydrous } H_3PO_4 - \text{mass of dry lignin} \left(\frac{MW_{PA}}{MW_L}\right)\right)}{\text{total mass}} \quad (22)$$

$$f_{LP,0} = \frac{\left(\text{mass of dry lignin} \left(\frac{MW_L + MW_{PA} - MW_W}{MW_L}\right)\right)}{\text{total mass}} \quad (23)$$

$$f_{WS,0} = \frac{\left(\text{mass of water} + \text{mass of dry lignin} \left(\frac{MW_{PA}}{MW_L}\right)\right)}{\text{total mass}} \quad (24)$$

The optimal values for the 12 unknown parameters in the model (k_{0j} , E_j , α' and MW_L) were estimated from the minimization of the least squares objective function F , Eq. (25), where n is the number of thermograms and $p(i)$ is the number of data points recorded for the i th thermogram (time, temperature fraction of the initial mass remaining and rate of mass loss). This objective function was chosen to simultaneously minimize the squared differences in the fraction of the initial mass remaining in the solid and the rate of mass loss. This was needed because it was observed that an objective function that was only based on the fraction of the initial mass gave optimal values that adjusted the data for the isothermal stages correctly, but gave poor results for the non-isothermal stages where the rates of mass loss were higher. Similarly, an objective function based on the rate of mass loss misrepresented the isothermal stages where the rate of mass loss was small.

The fraction of the initial mass remaining predicted by the model, $f(i, k)_{\text{model}}$, was calculated with Eqs. (13)–(21), which were integrated numerically by an explicit Euler method. The temperature recorded at each sampling time along the thermogram was used to calculate the instantaneous rate constants. The rates of mass loss were evaluated numerically from the values of $f(i, k)$. This method provided a sufficient degree of accuracy because, as the thermograms were recorded at a high sampling frequency (typically one data point every 4 s), the time increments used in the calculations were small

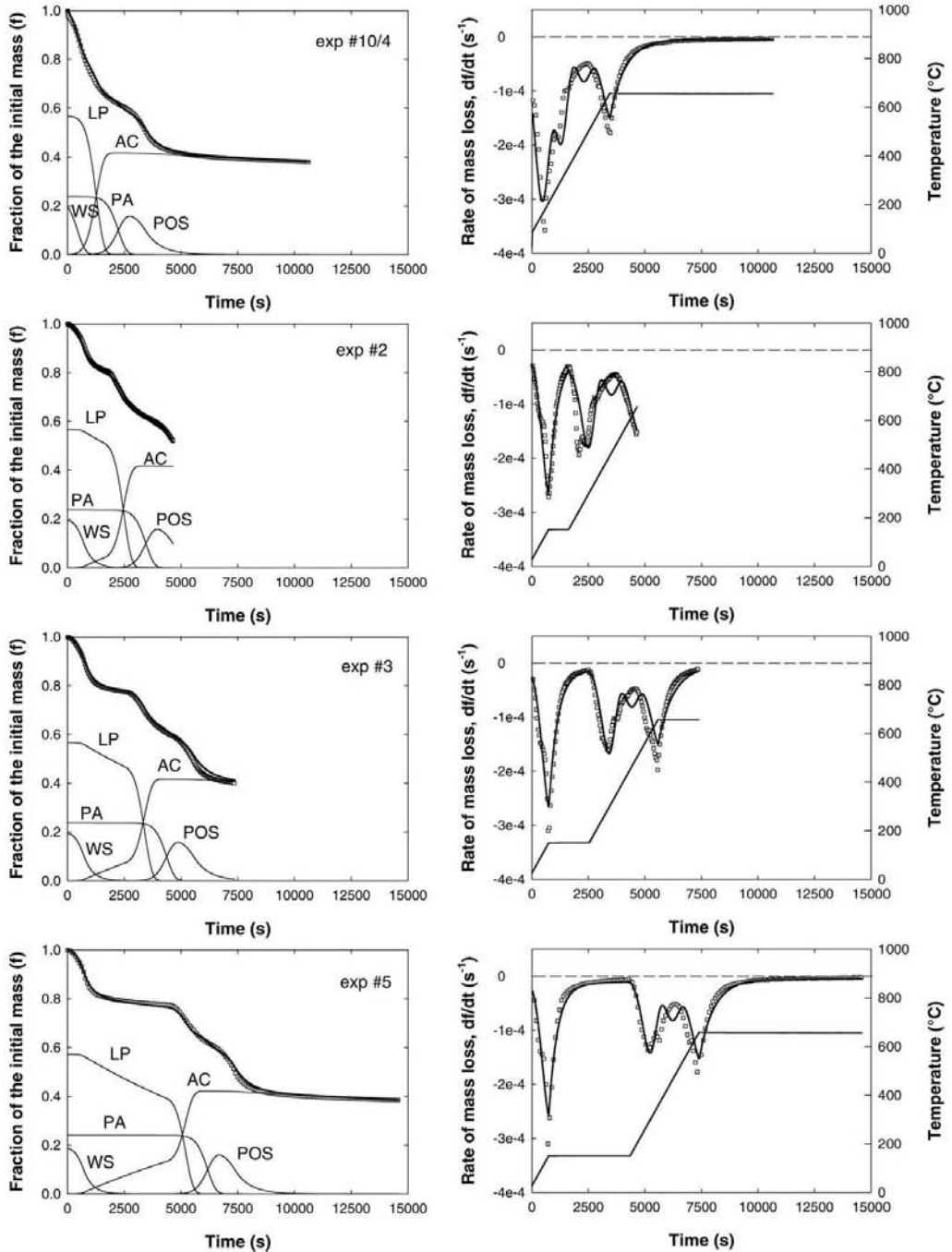


Fig. 3. Comparison between the experimental TG and DTG curves (□) and those calculated with the complete kinetic model (—), Eqs. (13)–(24), for experiments #2, #3, #5 and #10/4. (Experimental conditions listed in Table 2. Continuous thin lines are mass fractions calculated for lignin–phosphoric acid complex (LP), phosphoric acid (PA), water (WS), activated carbon (AC) and P_2O_5 (POS). For better visualization, only 1 data point out of 20 is plotted in the experimental TG and DTG curves.)

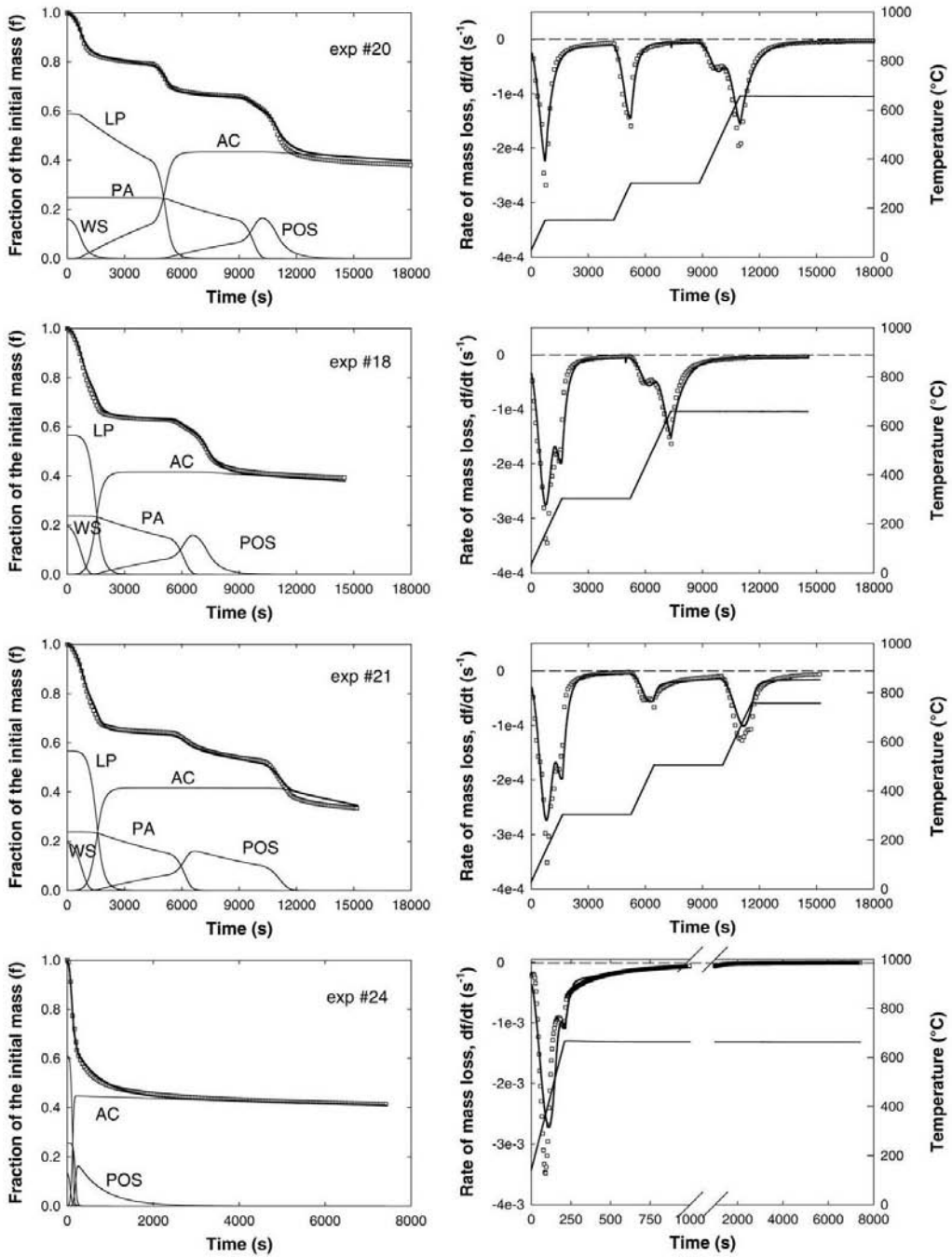


Fig. 4. Comparison between the experimental TG and DTG curves (\square) and those calculated with the two parallel reactions kinetic model ($-$), Eqs. (13)–(24), for experiments #18, #20, #21 and #24. (Experimental conditions listed in Table 2. Continuous thin lines are mass fractions calculated for lignin–phosphoric acid complex (LP), phosphoric acid (PA), water (WS), activated carbon (AC) and P_2O_5 (POS). For better visualization, only 1 data point out of 20 is plotted in the experimental TG and DTG curves.)

Table 3
 Least-squares best-fit values for the model parameters

Reaction	k_{0j} (s^{-1})	E_j (kJ/mol)	MW_L (g/mol)	α'	Minimum F
(2)	4.20	26.0	135.3	0.736	2.205×10^{-2}
(3)	395.9	72.0			
(4)	326.4	95.0			
(5)	73.9	47.7			
(6)	11.1	106.3			

enough to avoid numerical instability.

$$F = \left(\sum_{i=1}^n \left(\frac{\sum_{k=1}^{p(i)} \left(\frac{f(i,k)_{\text{experimental}} - f(i,k)_{\text{model}}}{f(i,k)_{\text{model}}} \right)^2}{p(i)} \right) \right)^{0.5} + \left(\sum_{i=1}^n \left(\frac{\sum_{k=1}^{p(i)} \left(\frac{\left(\frac{df(i,k)}{dt} \right)_{\text{experimental}} - \left(\frac{df(i,k)}{dt} \right)_{\text{model}}}{\left(\frac{df(i,k)}{dt} \right)_{\text{model}}} \right)^2}{p(i)} \right) \right)^{0.5} \quad (25)$$

The optimal values calculated for the activation energies (E_j), the frequency factors (k_{0j}), the stoichiometric coefficient in reaction (5) (α') and the apparent molar mass of lignin (MW_L) are shown in Table 3. Activation energies were 26.0 kJ/mol for water desorption, 72.0 kJ/mol for the dehydration of phosphoric acid to phosphoric pentoxide, 95.0 kJ/mol for the volatilization of P_2O_5 , 47.7 kJ/mol for the carbonization of the activated lignin and 106.3 kJ/mol for the pyrolytic release of light gases from activated carbon. The activation energy for the volatilization of lignin impregnated with phosphoric acid lies in the 35–100 kJ/mol range reported for lignin pyrolysis using several kinetic models [23], and falls below the range of activation energies from 60.6 kJ/mol at 200 °C to 153.6 kJ/mol at 700 °C reported for the pyrolysis of lignin activated with $ZnCl_2$ using a kinetic model based on a continuous distribution of activation energies [24]. Fig. 5 shows a sensitivity analysis for the influence of the model parameters on the least squares objective function F . This analysis shows that the activation energies (E_j), the apparent molar mass of lignin (MW_L) and the stoichiometric coefficient for the carbonization of the activated lignin (α') are evaluated accurately because the error function F is very sensitive to small variations in their individual values. The frequency factors (k_{0j}) that we have calculated are more uncertain due to the low sensitivity of the error function to their value, especially for the frequency factor for the rate constants of phosphoric acid dehydration (k_3) and water volatilization (k_2).

Figs. 3 and 4 compare the thermograms measured for the experiments at an 85% phosphoric acid-to-lignin mass ratio of 1.4:1 (Table 2), and those calculated with the model using the best-fit values of the parameters. Agreement between the model and the experiments is excellent for all the thermo-

grams, regardless of the number of intermediate isothermal stages. The same graphs also show the evolution of the mass fractions of water in the sample (WS), lignin-phosphoric acid complex (LP), phosphoric acid (PA), P_2O_5 (POS) and activated carbon (AC). Analysis of the temporal evolution of the mass fractions computed for each component in the solid mixture shows that drying of the sample (reaction (2)) takes place at the lowest temperature and is completed before the sample reaches 200 °C. Carbonization of the activated lignin (LP) starts at around 100 °C and is completed when the sample reaches 400 °C for the experiments without

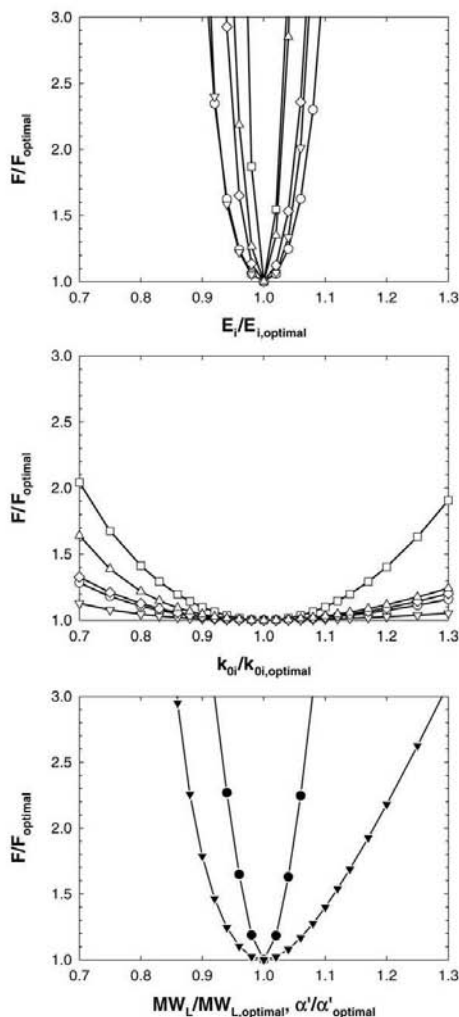


Fig. 5. Sensitivity analysis for the model parameters: activation energies (top), frequency factors (middle), and molar mass of lignin, MW_L , and α' (bottom) (E_1, k_1 : ○; E_2, k_2 : ▽; E_3, k_3 : □; E_4, k_4 : ◇; E_5, k_5 : △; α' : ▼; and MW_L : ●).

intermediate isothermal stages (experiment #10/4), or with an isothermal stage at 150 °C for 60 min (experiment #5), but reaches completion at 300 °C if an isothermal stage at 300 °C for 60 min is included in the temperature program (experiment #18). Decomposition and volatilization of the excess phosphoric acid take place at a higher temperature and are responsible for the mass loss observed above 400 °C. This starts at around 230 °C, which is close to the value of 213 °C reported for pure orthophosphoric acid [22], and is completed at around 550–580 °C. This broad interval of reaction temperature agrees qualitatively with the consecutive

reactions involved in the formation of P₂O₅ from phosphoric acid, which proceeds through the formation of pyrophosphoric acid (H₄P₂O₇), polyphosphoric acid (H_{n+2}P_nO_{3n+1}) and finally P₂O₅. The volatilization of phosphorous pentoxide also happens in a broad interval of temperature. According to the kinetic model, it starts once the sample reaches around 280 °C, which is close to its sublimation temperature of 300 °C, and takes place much faster above 570 °C when vaporization is accelerated due to the melting of P₂O₅ at 580–585 °C [22]. Finally, the residual mass loss during the isothermal stage at 650 °C is caused by the release of light

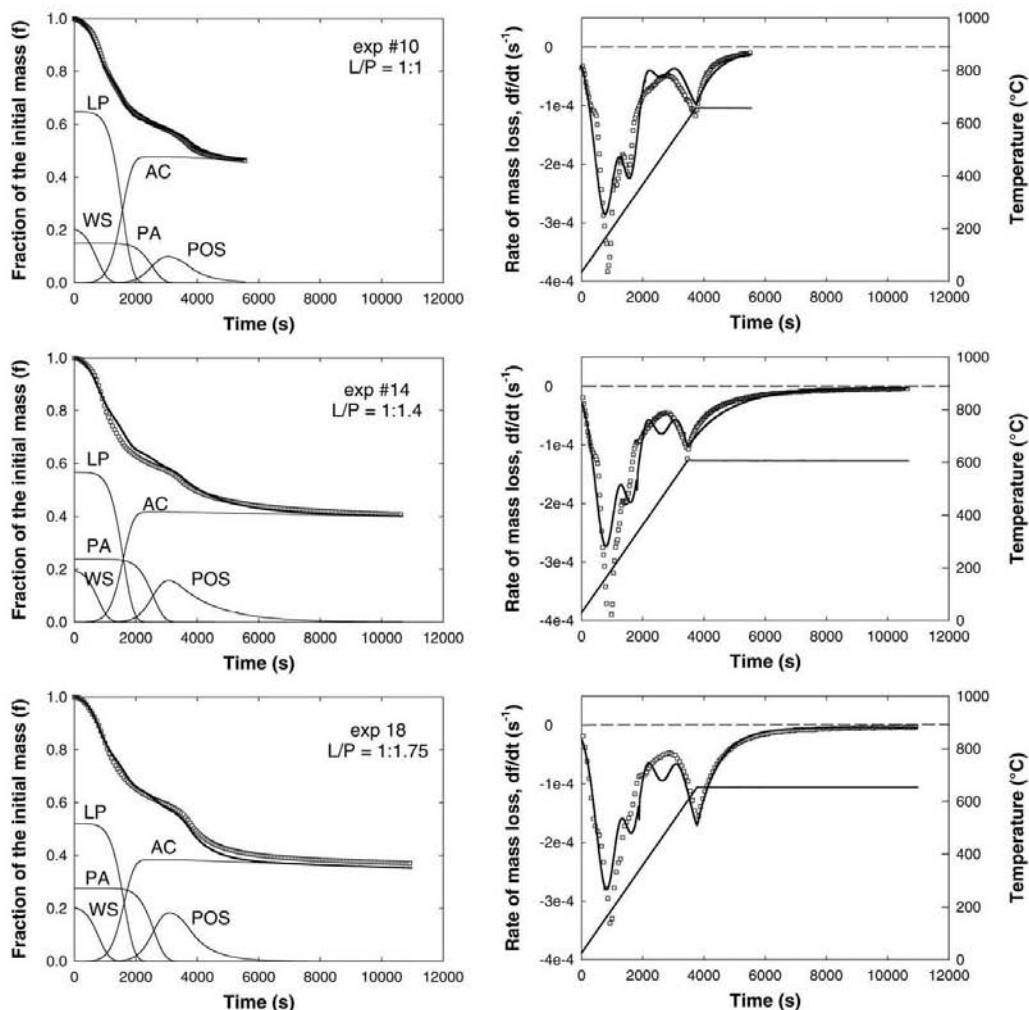


Fig. 6. Comparison between the experimental TG and DTG curves (□) and those calculated with the two parallel reactions kinetic model (—), Eqs. (13)–(24), for experiments #10 L/P 1:1.0, #14 L/P 1:1.4 and #18 L/P 1:1.75. (Experimental conditions listed in Table 2. Continuous thin lines are mass fractions calculated for lignin–phosphoric acid complex (LP), phosphoric acid (PA), water (WS), activated carbon (AC) and P₂O₅ (POS). For better visualization, only 1 data point out of 20 is plotted in the experimental TG and DTG curves.)

gases as the carbon formed at lower temperatures is pyrolyzed to a greater extent.

Analysis of the differential thermograms, also presented in Figs. 3 and 4, shows that the model accurately describes the rate of mass loss for the experiments with one intermediate isothermal stage at 300 °C (#18, #20, #21). Four maximums in the rate of weight loss are observed: the first for water volatilization, the second for the release of volatiles during the formation of activated carbon, the third for the decomposition of phosphoric acid and the fourth for the volatilization of P₂O₅. For the other experiments there are some discrepancies in the temperature interval from 300 to 500 °C since the model shows the existence of a small maximum on the rate of mass loss at around 450 °C caused by phosphoric acid dehydration to phosphorous pentoxide, which is not observed experimentally. Close examination of the experimental rate of mass loss in this temperature range shows a series of small maximums and inflection points (see experiments #2 and #3, for instance), which point to the existence of a set of simultaneous reactions taking place in the solid. These reactions are probably related to the decomposition of phosphoric acid to P₂O₅, which in the model has been assumed to proceed through a single reaction step (Eq. (9)), though, as described before, it actually proceeds through a series of consecutive steps (Fig. 5).

The influence of the PA-to-lignin ratio is examined in Fig. 6, which shows the results for experiments performed at PA-to-lignin ratios of 1.0:1.0, 1.4:1.0 and 1.75:1.0 (w:w) using similar temperature profiles throughout the experiment. The model can reproduce the measured thermograms within the limits of the experimental error in all cases, thus proving its robustness. Analysis of the differential thermograms show limitations for the three experiments similar to those noted earlier: the model can describe the general trends in the temporal evolution of the rate of mass loss but there are minor discrepancies in the temperature interval from 300 to 500 °C caused by the complex nature of the reactions involved in phosphoric acid decomposition.

5. Conclusions

A phenomenological kinetic model has been developed for the pyrolysis of lignin activated with phosphoric acid at low heating rates to produce activated carbon. The model is based on TG and DTG data from pyrolysis experiments and it assumes that lignin carbonization proceeds through a set of pseudo-first-order reactions. These reactions are a simplified description of the multiple reaction processes involved in the thermal decomposition of lignin mixed with an excess of phosphoric acid. The model provides a good representation of the thermograms regardless of the phosphoric-acid-to-lignin ratio and the temperature profile along the reaction. The activation energies and other parameters have been calculated from the experimental mass-loss and differential mass-loss curves. The model could be improved if the composition of

the volatile products were analyzed continuously by on-line mass spectrometry to determine the actual rates of volatilization for water, phosphoric acid-derived products (i.e., P₂O₅) and carbon-containing compounds.

Acknowledgements

The authors are indebted to the Catalan Regional Government and the Spanish Government for financial support (projects 2001SGR-00323 and PPQ2002-04201-CO2-02, respectively). Vanessa Torné-Fernández is grateful to the Rovira i Virgili University (URV) for a PhD scholarship.

References

- [1] T. Vemerson, P.R. Bonelli, E.G. Cerrella, A.L. Cukierman, *Arundo donax* cane as precursor for activated carbons preparation by phosphoric acid activation, *Biores. Technol.* 83 (2002) 95–104.
- [2] V.D. del Bagno, R.L. Miller, J.J. Watkins, On site production of activated carbon from Kraft Black Liquor, US EPA Report 600/2-78-191, 1978.
- [3] J. Rodríguez-Mirasol, T. Cordero, J.J. Rodríguez, Preparation and characterization of activated carbons from eucalyptus kraft lignin, *Carbon* 31 (1993) 87–95.
- [4] E. González Serrano, T. Cordero, J. Rodríguez-Mirasol, J.J. Rodríguez, Development of porosity upon chemical activation of Kraft lignin with ZnCl₂, *Ind. Eng. Chem. Res.* 36 (1997) 4832–4838.
- [5] H. Teng, T.S. Yeh, L.Y. Hsu, Preparation of activated carbon from bituminous coal with phosphoric acid activation, *Carbon* 36 (1998) 1387–1395.
- [6] J. Hayashi, A. Kazehaya, K. Muroyama, P. Watkinson, Preparation of activated carbon from lignin by chemical activation, *Carbon* 38 (2000) 1873–1878.
- [7] V. Fierro, V. Torné-Fernández, D. Montané, R. García-Valls, Removal of Cu (II) from aqueous solutions by adsorption on activated carbons prepared from Kraft lignin, in: A. Linares-Solano, D. Cazorla-Amorós (Eds.), *Proceedings of Carbon 2003*, Oviedo, Spain.
- [8] V. Fierro, V. Torné-Fernández, D. Montané, J. Salvadó, Activated carbons prepared from Kraft lignin by phosphoric acid impregnation, in: A. Linares-Solano, D. Cazorla-Amorós (Eds.), *Proceedings of Carbon 2003*, Oviedo, Spain.
- [9] S.H. Yoon, B.C. Kim, Y. Koral, I. Mochida, Multi-staged carbonization of aramid fibers, in: *Proceedings of the 22nd Biennial Conference on Carbon*, Extended Abstract and Program, San Diego, CA, 1995, p. 218.
- [10] C. Pastor, F. Rodríguez-Reinoso, H. Marsh, M.A. Martínez, Preparation of activated carbon cloths from viscous rayon. Part I. Carbonization procedures, *Carbon* 37 (1999) 1275–1283.
- [11] F. Suárez-García, A. Martínez-Alonso, J.M.D. Tascón, Pyrolysis of apple pulp: effect of operation conditions and chemical additives, *J. Anal. Appl. Pyrolysis* 62 (2002) 93–109.
- [12] G. Varhegyi, M.J. Antal, Kinetics of the thermal decomposition of cellulose, hemicellulose and sugar cane bagasse, *Energy Fuels* 3 (1989) 329–335.
- [13] J.J. Manyà, E. Velo, L. Puigjaner, Kinetics of biomass pyrolysis: a reformulated three-parallel-reactions model, *Ind. Eng. Chem. Res.* 42 (2003) 434–441.
- [14] J.A. Caballero, A. Marcilla, J.A. Conesa, Thermogravimetric analysis of olive stones with sulphuric acid treatment, *J. Anal. Appl. Pyrolysis* 44 (1997) 75–88.
- [15] J.J.M. Órfão, F.J.A. Antunes, J.L. Figueiredo, Pyrolysis kinetics of lignocellulosic materials - three independent reactions model, *Fuel* 78 (1999) 349–358.

- [16] J.J.M. Órfão, J.L. Figueiredo, A simplified method for determination of lignocellulosic materials pyrolysis kinetic from isothermal thermogravimetric experiments, *Thermochim. Acta* 380 (2001) 67–78.
- [17] D. Vamvuka, E. Kakaras, E. Kastanaki, P. Grammelis, Pyrolysis characteristics and kinetics of biomass residuals mixtures with lignite, *Fuel* 82 (2003) 1949–1960.
- [18] V. Cozzani, L. Petarca, L. Tognotti, Devolatilization and pyrolysis of refuse derived fuels: characterization and kinetic modeling by a thermogravimetric and calorimetric approach, *Fuel* 74 (1995) 903–912.
- [19] C.A. Koufopoulos, G. Maschio, A. Lucchesi, Kinetic modeling of the pyrolysis of biomass and biomass components, *Can. J. Chem. Eng.* 67 (1989) 75–84.
- [20] Y.Z. Lai, in: D.N.S. Hon, N. Shirashi (Eds.), *Chemical Degradation in Wood and Cellulose Chemistry*, vol. 10, Marcel Dekker, New York, 1991, p. 455.
- [21] M. Jagtoyen, F. Derbyshire, Activated carbons from yellow poplar and white oak by H_3PO_4 activation, *Carbon* 36 (1998) 1085–1097.
- [22] D.R. Lide (Ed.), *Handbook of Chemistry and Physics*, 72nd ed., CRC Press, Boca Raton, FL, 1991.
- [23] R.K. Sharma, J.B. Wooten, V.L. Baliga, X. Lin, W.G. Chan, M.R. Hajaligol, Characterization of chars from pyrolysis of lignin, *Fuel* (2004) (Corrected proof, available online 25 March).
- [24] E. Gonzalez-Serrano, $ZnCl_2$ —chemical activation of kraft lignin, PhD Dissertation, University of Málaga, Málaga, Spain, 1996.

5.1.2. Study of the decomposition of Kraft lignin impregnated with orthophosphoric acid

Este artículo se ha publicado en el journal Thermochemica Acta en 2005 en el volumen 433, páginas 142 a 148.



Study of the decomposition of kraft lignin impregnated with orthophosphoric acid

V. Fierro^{a,*}, V. Torné-Fernández^a, D. Montané^a, A. Celzard^b

^a *Departament de Enginyeria Química, Universitat Rovira i Virgili, Avda dels Països Catalans, 26, 43007 Tarragona, Spain*

^b *Laboratoire de Chimie du Solide Minéral, Université Henri Poincaré—Nancy I, UMR—CNRS 7555, BP 239, 54506 Vandœuvre-lès-Nancy, France*

Received 9 November 2004; received in revised form 18 February 2005; accepted 18 February 2005
Available online 24 March 2005

Abstract

The aim of this study was to analyze the pyrolysis of Kraft lignin impregnated with orthophosphoric acid by thermogravimetry (TG-DTG). We studied the effect of various parameters on both the char yield and the rate of mass loss: heat treatment temperature up to 650 °C, impregnation time, inclusion of isothermal periods, acid to lignin mass ratio (P/L) and gaseous atmosphere. Decomposition of pure lignin showed two maxima in the mass loss corresponding to evolution of moisture at 92 °C and to lignin decomposition in a broad temperature range from 150 to 650 °C, respectively. When orthophosphoric acid was added, lignin dehydration proceeded to a larger extent, decomposition occurred in a narrower temperature range and decomposition ended at lower temperatures with higher char yields. There was an optimum P/L at values between 0.8 and 1.0, and further increasing P/L had low influence on the decomposition mechanisms. Differential Thermal Analysis (DTA) showed that reactions occurring upon impregnation of lignin with orthophosphoric acid at room temperature are finished after only 1 h, which confirmed the TG-DTG results. Impregnation times longer than 1 h and inclusion of isothermal periods did not affect significantly the subsequent char yield. Concerning the gaseous atmosphere, identical char yield were obtained whether the samples be prepared in nitrogen or in air at 450 °C. However, decomposition in air at 650 °C produced a decrease in the char yield when compared to pyrolysis in nitrogen due to the evaporation of P₂O₅ and the subsequent oxidation of the unprotected carbon.
© 2005 Elsevier B.V. All rights reserved.

Keywords: Lignin; Activated carbon; H₃PO₄; Thermogravimetric analysis

1. Introduction

The kraft method produces black liquor, a residue composed by lignin (30–40%) and other inorganic compounds, that is used as in-house fuel for the recovery of both energy and residual inorganic matter. The trend towards larger plant capacities and the optimization of the pulping process to improve cost effectiveness have led to the plants producing more by-product lignin than the amount that is needed to cover their energy consumption. The separation of lignin after water evaporation of black liquor could be an alternative to its incineration. Lignin is a bountiful and renewable source and could represent an attractive field for future in-

dustrial chemistry (i.e., as a substitute in the formulation of phenol–formaldehyde resins and adhesives). Another interesting option among these potential uses for lignin is the production of activated carbons.

Several authors have reported the use of kraft lignin as activated carbon precursor. Del Bagno et al. [1] investigated char and activated carbon manufacture from black liquors at a pilot-plant scale. Rodríguez-Mirasol et al. [2] prepared activated carbons from carbonization of eucalyptus kraft lignin. The latter research group also studied the chemical activation of this precursor by using ZnCl₂ [3] and obtained microporous activated carbons with a BET surface area as high as 1800 m² g⁻¹. However, the use of ZnCl₂ has declined due to the environmental problems [4] and orthophosphoric acid (PA) is preferred as activating-dehydrating agent.

* Corresponding author. Tel.: +34 977 558546; fax: +34 977 558544.
E-mail address: vanessa.fierro@urv.net (V. Fierro).

PA promotes the bond cleavage in the biopolymers and dehydration at low temperatures [5], followed by extensive cross-linking that bonds volatile matter into the carbon product and so an increase in carbon yield. Benadi et al. [6] showed that the mechanism of PA activation of biomass feedstocks occurs through various steps: cellulose depolymerization, biopolymers dehydration, formation of aromatic rings and elimination of phosphate groups. This allows activated carbons to be prepared with good yields and high surface areas.

The use of PA as activating agent has been reported with various agricultural by-products [7–20], wood [21,22], natural carbons [4,23,24] and synthetic carbons [25,26]. As far as we know, there is only one paper wherein the possibility of chemical activation of kraft lignin with PA among other activating agents has been examined [27]. The authors carried out carbonization over the temperature range of 500–900 °C held for 1 h and under N₂ flow: maximum surface areas of more than 1300 m² g⁻¹ were found at 600 °C.

This paper deals with the thermal decomposition of kraft lignin activated with PA in order to analyze the effect of the operation conditions on the char yield and on the rate of mass loss. The operation conditions studied were the impregnation time, the inclusion of isothermal periods, the PA to lignin mass ratio and the gaseous atmosphere. The role of PA as activating agent but also as inhibitor of carbon oxidation are herein analyzed.

2. Experimental

Kraft lignin was provided by Lignotech Iberica S.A. (Spain). Table 1 shows the proximate and ultimate analysis of lignin. The proximate analysis was carried out according to ISO standards following the weight losses at 100 °C/air (moisture), 900 °C/non-oxidizing atmosphere (volatile matter) and 815 °C/air (ash). An 85 wt.% H₃PO₄ aqueous solution (Panreac, Spain) was used as activating agent. Ultimate analysis was carried out in a EA1108 Carlo Erba Elemental Analyser. Results presented in Table 1 are very similar to those already reported [28].

Table 1
Lignin analysis (wt.%)

Proximate analysis (wt.%, wet basis)	
Moisture	14.5
Ash	9.5
Volatile matter	45.0
Fixed carbon ^a	31.0
Ultimate analysis (wt.%, ash and moisture free)	
Carbon	59.5
Hydrogen	5.1
Nitrogen	0.1
Sulphur	2.2
Oxygen ^a	33.1

^a Estimated by difference.

Lignin was mixed with varying amounts of H₃PO₄ in the range of 0.3–1.8 PA to lignin mass ratio (P/L). The slurry was left for impregnation times from 1 to 22 h at room temperature and under air, then transferred to a Perkin-Elmer TGA 7 thermobalance wherein decomposition was carried out at temperatures up to 650 °C. In this study, approximately 30–50 mg of sample was heated up to a maximum temperature of 650 °C and in a flow rate of 50 cm³ min⁻¹ measured at room temperature and atmospheric pressure.

Experiments were repeated three times to be sure of the reproducibility, which was found to be quite satisfactory. Average data obtained at each set of operation conditions were considered for results and discussion. For comparison purposes between the various activation parameters, we used a sample impregnated for 1 h with a P/L of 1.4 and pyrolyzed with a heating rate of 10 °C min⁻¹ up to 650 °C in nitrogen. The operation conditions were varied with regard to this reference. The effect of impregnation time was studied for samples left for 1 and 22 h at room temperature. The inclusion of isothermal periods was studied holding temperature for 15, 30 or 60 min at 150 °C or for 60 min at 300 °C and heating the sample at 10 °C min⁻¹ up to 650 °C afterwards. The effect of P/L was studied for samples with a P/L of 0.3, 0.6, 0.8, 1.0, 1.4 and 1.8. Finally, the effect of gas atmosphere on decomposition was studied using nitrogen or air and heating the sample to a maximum temperature of either 450 or 650 °C, which temperatures were held for 120 min.

Differential thermal analysis (DTA) was performed by simply recording the voltage drop at both ends of a differential chromel–alumel thermocouple, having one temperature probe embedded within the 1.4 P/L mixture (i.e., the sample), while the other one was inside a fine powder of dry α -alumina (i.e., the reference). The experiment was carried out at room temperature, and the P/L mixture was stirred by the thermocouple probe itself. For that purpose, any part of the experiment (thermocouple, sample and reference), was handled using metallic tongs, in order to avoid parasitic heating due to the fingers of the operator.

3. Results and discussion

Fig. 1(a) and (b) shows thermogravimetric (TG) and differential thermogravimetric (DTG) curves, respectively, for pure lignin, PA and 0.3 P/L mixture when heated at 10 °C min⁻¹ up to a temperature of 650 °C in nitrogen. The three samples were next maintained 2 h long at this latter final temperature. At the initial stage of the thermal treatment, pure lignin losses moisture from room temperature (T_{1a}) to 131 °C (T_{1b}). The dehydration proceeds with a maximum rate at 60 °C (T_{1max}), reaching a constant weight of 87% at 131 °C. Degradation of pure lignin occurs over a broad temperature interval (150–650 °C), with a maximum weight-loss rate between 300 and 370 °C. The decomposition of lignin is highly complex and depends on several factors such as its origin. The occurrence of lignin degradation in a wide range of temperatures